



# CHORUS

This is the accepted manuscript made available via CHORUS. The article has been published as:

## Validity of Factorization of the High-Energy Photoelectron Yield in Above-Threshold Ionization of an Atom by a Short Laser Pulse

M. V. Frolov, D. V. Knyazeva, N. L. Manakov, A. M. Popov, O. V. Tikhonova, E. A. Volkova, Ming-Hui Xu, Liang-You Peng, Liang-Wen Pi, and Anthony F. Starace

Phys. Rev. Lett. **108**, 213002 — Published 22 May 2012

DOI: [10.1103/PhysRevLett.108.213002](https://doi.org/10.1103/PhysRevLett.108.213002)

# On the Validity of Factorization of the High-Energy Photoelectron Yield in Above-Threshold Ionization of an Atom by a Short Laser Pulse

M. V. Frolov,<sup>1,2</sup> D. V. Knyazeva,<sup>1</sup> N. L. Manakov,<sup>1,\*</sup> A. M. Popov,<sup>3,†</sup> O. V. Tikhonova,<sup>3</sup> E. A. Volkova,<sup>3</sup> Ming-Hui Xu,<sup>4</sup> Liang-You Peng,<sup>4,2,‡</sup> Liang-Wen Pi,<sup>5,2</sup> and Anthony F. Starace<sup>5,2,§</sup>

<sup>1</sup>*Department of Physics, Voronezh State University, Voronezh 394006, Russia*

<sup>2</sup>*Kavli Institute for Theoretical Physics China, CAS, Beijing 100190, China*

<sup>3</sup>*D.V. Skobeltsyn Institute of Nuclear Physics, M.V. Lomonosov Moscow State University, Moscow 199991, Russia*

<sup>4</sup>*State Key Laboratory for Mesoscopic Physics and Department of Physics, Peking University, Beijing 100871, China*

<sup>5</sup>*Department of Physics and Astronomy, The University of Nebraska, Lincoln NE 68588-0299, USA*

An analytic description for the yield,  $\mathcal{P}(\mathbf{p})$ , of high-energy electrons ionized from an atom by a short (few-cycle) laser pulse is obtained quantum mechanically. Factorization of  $\mathcal{P}(\mathbf{p})$  in terms of an electron wave packet and the cross section for elastic electron scattering (EES) is shown to occur only for an ultrashort pulse, while in general  $\mathcal{P}(\mathbf{p})$  involves interference of EES amplitudes with laser-field-dependent momenta. The analytic predictions agree well with accurate numerical results.

PACS numbers: 32.80.Rm, 34.50.Rk, 42.50.Hz, 42.65.Re

The process of above-threshold ionization (ATI) by a short (few-cycle) laser pulse is highly sensitive to the parameters of the pulse, whose vector potential  $\mathbf{A}(t)$  (for the case of linear polarization) may be parameterized as:

$$\mathbf{A}(t) = \hat{\mathbf{z}}A(t), \quad A(t) = f(t) \sin(\omega t + \phi), \quad (1)$$

where  $f(t)$  is the pulse envelope (with its maximum at  $t = 0$ ),  $\omega$  is the carrier frequency, and  $\phi$  is the carrier-envelope phase (CEP). The first ATI experiments with CEP-stabilized short pulses [1] found a significant CEP-dependence of the electron yield and differences in the energy extent of the ATI plateau for electrons with negative and positive momentum projections  $p_{\parallel} = \mathbf{p} \cdot \hat{\mathbf{z}} = p \cos \theta$ . More detailed measurements [2] found CEP-dependent interference fringes (differing for electrons with  $p_{\parallel} < 0$  and  $p_{\parallel} > 0$ ) in angle-resolved ATI spectra produced by different half-cycles of a few-cycle pulse. These peculiarities have been confirmed by numerical solutions of the time-dependent Schrödinger equation (TDSE) and explained within the improved strong field approximation, in which the atomic potential  $U(r)$  is taken into account perturbatively, in a Born-like approximation [3]. However, recent experiments [4] show that a perturbative treatment of  $U(r)$  is inadequate to extract from ATI spectra information on atomic dynamics, such as the field-free differential cross section (DCS) for elastic electron scattering (EES) from the potential  $U(r)$ . The phenomenological factorization of the ATI yield in terms of an electron wave packet (EWP) and the *exact* (non-Born) DCS for EES [5, 6] is very useful for analyzing signatures of atomic dynamics in ATI spectra. For a monochromatic field, this factorization was justified theoretically in Ref. [7] [cf. also Ref. [8] in which this factorization was introduced heuristically (as the authors state in a later paper [9])]. For a one-dimensional zero-range potential model, analytic derivations of the ATI yield for an arbitrary shape of  $A(t)$  have been performed in Ref. [10] using an adiabatic approach. However, the validity of

a factorized formula for the ATI yield for a short pulse with stabilized CEP, suggested in Ref. [11], remains unjustified theoretically, and is a challenge for theory.

In this Letter we present an analytic description of ATI by a few-cycle, CEP-stabilized laser pulse. Our closed-form analytic formulas show that the photoelectron yield, in general, cannot be factorized into the product of an EWP and the DCS for EES, but involves a sum of DCSs with different (pulse shape-dependent) electron momenta as well as interference between corresponding EES amplitudes. Only in the ultrashort pulse case (in which only electrons ionized by a *single optical cycle* of the pulse contribute significantly to the photoelectron yield) do our results reduce to factorized form. For the H and He atoms, our TDSE results confirm the high accuracy of our analytic description of high-energy ATI plateau.

To describe ATI by a short laser pulse, we generalize our analytic description of ATI plateau spectra produced by a monochromatic field [7] in a way similar to that used to describe harmonic generation by a short pulse [12]. The key idea is to consider first ATI by an infinite train of short pulses (1) separated in time by  $\mathcal{T}$  with  $\mathcal{T} > \tau$ , where  $\tau$  is the duration of the single short pulse (1) whose ATI spectrum we seek. Owing to the periodicity in time of the pulse train, we can employ the quasistationary quasienergy state approach [13] to obtain an *ab initio* formulation for the differential  $n$ -photon ionization rates  $\Gamma(\mathbf{p}_n) \equiv d\Gamma(\mathbf{p}_n)/d\Omega_{\mathbf{p}_n}$  in a periodic field of frequency  $\omega_{\mathcal{T}} = 2\pi/\mathcal{T}$ , where  $\mathbf{p}_n$  is the photoelectron momentum. The total ionization probability for the period  $\mathcal{T}$  is:

$$P = \mathcal{T}\Gamma = \frac{2\pi}{\omega_{\mathcal{T}}} \sum_{n>n_0} \int \Gamma(\mathbf{p}_n) d\Omega_{\mathbf{p}_n}, \quad (2)$$

where  $n_0$  is the minimum number of photons for ionization from a bound state of energy  $E_0 = -\hbar^2\kappa^2/(2m)$ . In the limit  $\mathcal{T} \rightarrow \infty$  ( $\omega_{\mathcal{T}} \rightarrow 0$ ), the sum over  $n$  in Eq. (2) can be replaced by an integral over the electron's momentum

$p_n \equiv p$  or energy  $E = p^2/(2m)$ . The result we obtain is:

$$P = \int \int \mathcal{P}(\mathbf{p}) dE d\Omega_{\mathbf{p}},$$

where the doubly differential ionization probability,  $\mathcal{P}(\mathbf{p})$ , for a *single short pulse* has the following form:

$$\mathcal{P}(\mathbf{p}) \equiv \frac{d^2 P}{dE d\Omega_{\mathbf{p}}} = \lim_{\omega_r \rightarrow 0} \frac{2\pi}{\hbar\omega_r^2} \Gamma(\mathbf{p}). \quad (3)$$

For an electron in a short-range potential  $U(r)$ , the rate  $\Gamma(\mathbf{p})$  can be obtained (using time-dependent effective range theory [14]) in analytic form in the tunneling limit. This latter result can then be straightforwardly generalized to the case of an active atomic electron, as in Ref. [7]. Our analysis shows that the ATI amplitude  $\mathcal{A}(\mathbf{p})$  for a short pulse can be presented as a sum of partial amplitudes,  $\mathcal{A}_j(\mathbf{p})$ , describing electrons ionized at each  $j$ th ( $j = 1, 2, \dots, 2N$ ) optical half-cycle  $T/2 = \pi/\omega$  of the  $N$ -cycle pulse (1). In the low-frequency limit ( $\hbar\omega \ll |E_0|$ ), these amplitudes can be estimated using a modified saddle-point analysis, as done similarly in Ref. [7]. As a result, the amplitudes  $\mathcal{A}_j(\mathbf{p})$  depend on tunneling ionization ( $t_i^{(j)}$ ) and rescattering ( $t_r^{(j)}$ ) times for the  $j$ th *half-cycle* [where  $t_r^{(j)}$  lies in the  $(j+1)$ th half-cycle], which satisfy the system of classical equations:

$$\begin{aligned} A(t_i^{(j)}) - \frac{1}{t_r^{(j)} - t_i^{(j)}} \int_{t_i^{(j)}}^{t_r^{(j)}} A(t) dt &= 0, \\ 2F(t_r^{(j)}) + \frac{1}{c} \frac{A(t_r^{(j)}) - A(t_i^{(j)})}{t_r^{(j)} - t_i^{(j)}} &= 0, \end{aligned} \quad (4)$$

where  $\hat{\mathbf{z}}F(t)$  is the electric field of the pulse [ $F(t) = -(1/c)dA/dt$ ]. The desired solutions ( $t_i^{(j)}, t_r^{(j)}$ ) of the system (4) are those real solutions that ensure the shortest return time,  $\Delta t_j = (t_r^{(j)} - t_i^{(j)}) < T$ , and the maximum classical energy,  $\mathcal{E}_{\max,j}^{(\text{cl})}$ , gained by an electron from the laser field over the time  $\Delta t_j$ . With known  $t_i^{(j)}$  and  $t_r^{(j)}$ , the amplitude  $\mathcal{A}_j(\mathbf{p})$  can be approximated in a way similar to that for a monochromatic field [7]. Moreover, for positive (or negative)  $p_{||}$  only those partial amplitudes  $\mathcal{A}_j(\mathbf{p})$  contribute for which  $F(t_i^{(j)}) < 0$  [or  $F(t_i^{(j)}) > 0$ ].

Omitting technical details, we focus here on the final analytic result for  $\mathcal{P}(\mathbf{p})$ , which involves two terms:

$$\mathcal{P}(\mathbf{p}) = \mathcal{P}_{\text{dir}}(\mathbf{p}) + \mathcal{P}_{\text{int}}(\mathbf{p}). \quad (5)$$

The first (“direct”) term is the sum of partial rates  $\Gamma_j(\mathbf{p})$ :

$$\mathcal{P}_{\text{dir}}(\mathbf{p}) = \frac{2\pi}{\hbar\omega^2} \sum_j' \Gamma_j(\mathbf{p}), \quad (6)$$

where the prime on the sum means that the summation is taken over  $j$  of the same (even or odd) parity depending

on the sign of  $p_{||}$ . The rate  $\Gamma_j(\mathbf{p})$  describes photoelectrons created by the  $j$ th half-cycle of the pulse and can be represented as a product of three factors similar to that for a monochromatic field [7]:

$$\Gamma_j(\mathbf{p}) = \mathcal{I}_j \mathcal{W}_j \sigma(\mathbf{p} - \Delta\mathbf{p}_j), \quad \Delta\mathbf{p}_j = -|e|\mathbf{A}(t_r^{(j)})/c. \quad (7)$$

The tunneling factor  $\mathcal{I}_j$  describes the tunneling of an active atomic electron at the moment  $t_i^{(j)}$ :

$$\mathcal{I}_j = \frac{m}{\pi\hbar\kappa} \tilde{\gamma}_j^2 \Gamma_{\text{st}}(\tilde{F}_j), \quad (8)$$

where  $\tilde{F}_j = |F(t_i^{(j)})|$ ,  $\tilde{\gamma}_j = \hbar\omega/(|e|\tilde{F}_j\kappa^{-1})$  is an effective value of the Keldysh parameter for the  $j$ th half-cycle, and  $\Gamma_{\text{st}}(\tilde{F}_j)$  is the tunneling rate for a bound atomic electron in an effective static electric field  $\hat{\mathbf{z}}F(t_i^{(j)})$  [15]. The factor  $\mathcal{W}_j$  in Eq. (7) describes the propagation of the electron in the laser-dressed continuum between the tunneling and rescattering events and involves the Airy function  $\text{Ai}(x)$ :

$$\mathcal{W}_j = \frac{p}{\hbar} \frac{\text{Ai}^2(\xi_j)}{\zeta_j^{2/3} \Delta t_j^3 \omega_{\text{at}}^2}, \quad \xi_j = \frac{\Delta E_j}{\zeta_j^{1/3} E_{\text{at}}}, \quad (9)$$

where  $E_{\text{at}} = \hbar\omega_{\text{at}} = e^2/a$ ,  $a$  is the Bohr radius,

$$\Delta E_j = \frac{(\mathbf{p} - \Delta\mathbf{p}_j)^2}{2m} - \mathcal{E}_{\max,j}^{(\text{cl})} + 2|E_0| \frac{F(t_r^{(j)})}{F(t_i^{(j)})},$$

$$\mathcal{E}_{\max,j}^{(\text{cl})} = \frac{e^2 \left[ A(t_r^{(j)}) - A(t_i^{(j)}) \right]^2}{2mc^2},$$

$$\begin{aligned} \zeta_j &= \frac{1}{F_{\text{at}}^2} \left\{ -\frac{\dot{F}(t_r^{(j)})}{2|e|} \left[ p_{||} + \frac{|e|}{c} A(t_i^{(j)}) \right] + F^2(t_r^{(j)}) \right. \\ &\times \left. \left[ 4 \frac{F(t_r^{(j)})}{F(t_i^{(j)})} - 3 \right] \right\}, \quad F_{\text{at}} = \frac{|e|}{a^2}, \quad \dot{F}(t_r^{(j)}) \equiv \frac{dF(t)}{dt} \Big|_{t=t_r^{(j)}}. \end{aligned}$$

The factor  $\sigma(\mathbf{p} - \Delta\mathbf{p}_j)$  in Eq. (7) is the field-free DCS for EES from the atomic core with energy  $E_r = (\mathbf{p} - \Delta\mathbf{p}_j)^2/(2m)$  and scattering angle  $\Theta = \pi - \theta_r$ , where

$$\cos \theta_r = |(\mathbf{p} - \Delta\mathbf{p}_j) \cdot \hat{\mathbf{z}}|/|\mathbf{p} - \Delta\mathbf{p}_j|. \quad (10)$$

For the H atom,  $\sigma(\mathbf{p} - \Delta\mathbf{p}_j)$  is known analytically,

$$\sigma(\mathbf{p} - \Delta\mathbf{p}_j) = \frac{m^2 e^4}{(\mathbf{p} - \Delta\mathbf{p}_j)^4} (1 + \cos \theta_r)^{-2}, \quad (11)$$

while for other atoms experimental or theoretical data for  $\sigma(\mathbf{p})$  should be used, substituting there  $\mathbf{p} \rightarrow (\mathbf{p} - \Delta\mathbf{p}_j)$ .

The term  $\mathcal{P}_{\text{int}}(\mathbf{p})$  in Eq. (5) originates from the interference between the half-cycle ionization amplitudes  $\mathcal{A}_j(\mathbf{p})$  and  $\mathcal{A}_{j'}(\mathbf{p})$  having the same parity of  $j$  and  $j'$ . It thus involves their phase difference  $\Phi_{j,j'}$ :

$$\mathcal{P}_{\text{int}} = \frac{2\pi}{\hbar\omega^2} \sum_{j \neq j'}' s_{j,j'} \sqrt{\Gamma_j(\mathbf{p}) \Gamma_{j'}(\mathbf{p})} \cos \Phi_{j,j'}(\mathbf{p}), \quad (12)$$

$$\Phi_{j,j'} = \varphi_j - \varphi_{j'} + \psi(\mathbf{p} - \Delta\mathbf{p}_j) - \psi(\mathbf{p} - \Delta\mathbf{p}_{j'}), \quad (13)$$

$$\hbar\varphi_j = S_{\mathbf{p}}(t_r^{(j)}) - \int_{t_i^{(j)}}^{t_r^{(j)}} \left[ \mathcal{E}(t, t_i^{(j)}) - E_0 \right] dt, \quad (14)$$

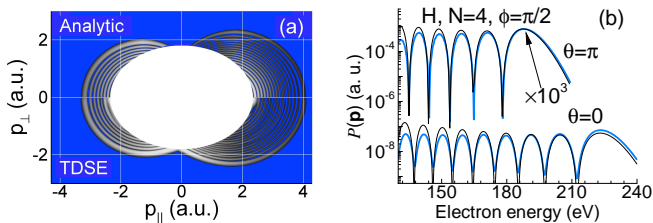


FIG. 1. (color online) (a): The momentum distribution  $\mathcal{P}(p_{\parallel}, p_{\perp})$  of electrons ionized from the H atom by a four-cycle  $\cos^2$ -shaped pulse with wavelength  $\lambda = 1.3 \mu\text{m}$ , peak intensity  $1.5 \times 10^{14} \text{ W/cm}^2$ , and CEP  $\phi = 0$ . Analytic (upper half-panel) and TDSE results (bottom half-panel) are shown for electron momenta at the high-energy end of the ATI plateau, i.e., outside the white ellipse centered at  $p_{\parallel} = p_{\perp} = 0$ . (b): ATI spectra for the laser pulse as in (a) but for  $\phi = \pi/2$  and  $\theta = 0$  and  $\pi$ . Thin (black) lines: Eq. (5); thick (blue) lines: TDSE results. Data for  $\theta = \pi$  have been multiplied by  $10^3$ .

$$S_{\mathbf{p}}(t_r^{(j)}) = \int_{-t_r^{(j)}}^{t_r^{(j)}} \frac{[\mathbf{p} + |e|\mathbf{A}(t)/c]^2}{2m} dt,$$

$$\mathcal{E}(t, t_i^{(j)}) = \frac{e^2}{2mc^2} \left[ A(t) - \frac{1}{t - t_i^{(j)}} \int_{t_i^{(j)}}^t A(\tau) d\tau \right]^2,$$

where  $s_{j,j'} = \text{sign}[\text{Ai}(\xi_j)\text{Ai}(\xi_{j'})]$  ( $= \pm 1$ ), and  $\psi(\mathbf{p})$  is the phase of the EES amplitude  $f(\mathbf{p})$ :

$$f(\mathbf{p}) = |f(\mathbf{p})|e^{i\psi(\mathbf{p})}. \quad (15)$$

In Figs. 1 and 2 we compare our analytic predictions for the probability  $\mathcal{P}(\mathbf{p})$  with numerical TDSE results for the case of a pulse (1) having a  $\cos^2$ -shaped envelope:

$$f(t) = -\frac{cF}{\omega} \cos^2\left(\frac{t\pi}{\tau}\right), \quad t \in [-\tau/2, \tau/2], \quad (16)$$

where  $\tau = 2\pi N/\omega$ . The peak intensity of the pulse is defined as  $I = cF^2/(8\pi)$ . The 3D TDSE for the H atom was solved using two different numerical algorithms, which provide the same results for the ATI spectra. (For details of the numerical solution of the TDSE for ATI, see Refs. [16, 17].) For He, we used the single active electron approximation with the same one-electron potential as in Ref. [18]. [This potential was also used to calculate  $f(\mathbf{p})$  and  $\sigma(\mathbf{p})$  for He.] The result (5) for  $\mathcal{P}(\mathbf{p})$  agrees well with the TDSE results, as shown in Figs. 1 and 2(a,b) for the H atom [for pulses with  $N = 4$  and 6, whose full widths at half maximum (FWHM) of the intensity are 6.3 and 9.5 fs, with  $T = 4.3$  fs] and in Figs. 2(c,d) for He for a six-cycle pulse (with FWHM of 5.8 fs,  $T = 2.67$  fs).

Both the momentum distribution  $\mathcal{P}(p_{\parallel}, p_{\perp})$  in Fig. 1(a) and the ATI spectra in Figs. 1(b) and 2 exhibit a left-right asymmetry [3], which in our analysis originates from different contributions to  $\mathcal{P}(\mathbf{p})$  of half-cycles with  $F(t) < 0$  and  $F(t) > 0$ . Indeed, electrons with  $p_{\parallel} > 0$  are created by half-cycles with  $F(t) < 0$ , while those with  $p_{\parallel} < 0$  by

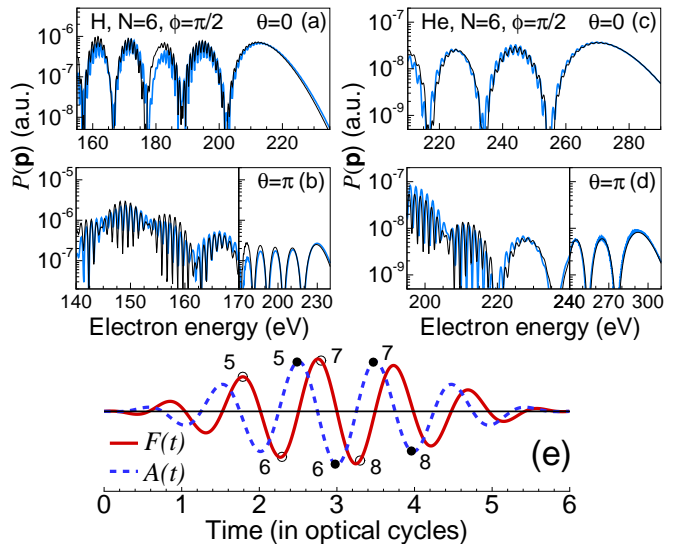


FIG. 2. (color online). ATI spectra produced by a six-cycle  $\cos^2$ -shaped pulse with  $\phi = \pi/2$  for (a,b) hydrogen (for  $\lambda = 1.3 \mu\text{m}$ ,  $I = 1.5 \times 10^{14} \text{ W/cm}^2$ ,  $u_p = 23.7 \text{ eV}$ ) and (c,d) helium (for  $\lambda = 0.8 \mu\text{m}$ ,  $I = 5 \times 10^{14} \text{ W/cm}^2$ ,  $u_p = 29.9 \text{ eV}$ ).  $\theta = 0$  in (a,c) and  $\theta = \pi$  in (b,d). Thin (black) lines: Eq. (5); thick (blue) lines: TDSE results. (e): Time evolution of  $F(t)$  and  $A(t)$  for a six-cycle  $\cos^2$ -shaped pulse with  $\phi = \pi/2$ . Open (solid) circles mark the positions of times  $t_i^{(j)}$  ( $t_r^{(j)}$ ), with the numbers marking the index  $j$  of the contributing half-cycle.

half-cycles with  $F(t) > 0$ . Moreover, due to the pulse-shape and CEP dependences of  $A(t)$  and  $F(t)$ , the times  $t_i^{(j)}$ ,  $t_r^{(j)}$  and the energies  $\mathcal{E}_{\text{max},j}^{(\text{cl})}$  are different for different  $j$ , resulting in different maximal energies of electrons (or plateau cutoff positions),  $E_{\text{cut}}^{(j)}$ , for half-cycles with different  $j$ ; e.g., for the case  $\theta = 0$  or  $\pi$ :

$$E_{\text{cut}}^{(j)} = \left( |\Delta \mathbf{p}_j|/\sqrt{2m} + \sqrt{\mathcal{E}_{\text{max},j}^{(\text{cl})}} \right)^2. \quad (17)$$

For  $p_{\parallel} > 0$  ( $p_{\parallel} < 0$ ) in Fig. 1(b) the major contribution to  $\mathcal{P}(\mathbf{p})$  comes from the single half-cycle with  $j = 4$  ( $j = 5$ ), for which  $E_{\text{cut}}^{(4)} \approx 9.4u_p$  ( $E_{\text{cut}}^{(5)} \approx 8.0u_p$ ), where  $u_p = e^2 F^2/(4m\omega^2) = 23.7 \text{ eV}$ . Hence, for the ATI spectra in Fig. 1(b),  $\mathcal{P}(\mathbf{p}) \approx \mathcal{P}_{\text{dir}}(\mathbf{p})$  has a factorized form (with EWP  $w_4$  for  $p_{\parallel} > 0$  and  $w_5$  for  $p_{\parallel} < 0$ ).

The large-scale interference minima in the ATI spectra in Figs. 1(b) and 2 originate from interference of two (short and long) electron trajectories [that contribute to the partial amplitudes  $\mathcal{A}_j(\mathbf{p})$ ]; they are similar to those for a monochromatic field [7, 19]. Besides these “intracycle” oscillations, there are fine-scale modulations of  $\mathcal{P}(\mathbf{p})$  that have a period  $\Delta E$  of order  $\hbar\omega$  and are characteristic for a short pulse [3], as seen clearly in Fig. 2. These “intercycle” oscillations originate from the interference term  $\mathcal{P}_{\text{int}}(\mathbf{p})$  in Eq. (5) and become pronounced for pulses with  $N > 4$ , when two adjacent partial rates,  $\Gamma_j(\mathbf{p})$  and  $\Gamma_{j+2}(\mathbf{p})$ , have different, large magnitudes. In Figs. 2(a,b)

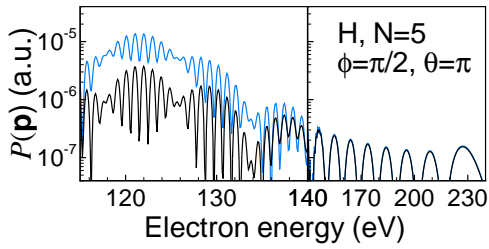


FIG. 3. H atom ATI spectra for the laser pulse of Fig. 2(b) with  $N = 5$ . Lower (black) curve: Eq. (5) result. Upper (blue) curve: approximate factorized formula result (cf. text).

the two are  $\Gamma_6(\mathbf{p})$  and  $\Gamma_8(\mathbf{p})$  with  $E_{\text{cut}}^{(6)} \approx 9.7u_p$  and  $E_{\text{cut}}^{(8)} \approx 6.3u_p$  for  $p_{\parallel} > 0$ , and  $\Gamma_5(\mathbf{p})$  and  $\Gamma_7(\mathbf{p})$  with  $E_{\text{cut}}^{(5)} \approx 8.0u_p$  and  $E_{\text{cut}}^{(7)} \approx 9.0u_p$  for  $p_{\parallel} < 0$  [cf. Fig. 2(e)]. Since for  $\theta = 0$  in Fig. 2(a) the cutoff energies and rates  $\Gamma_5(\mathbf{p})$  and  $\Gamma_7(\mathbf{p})$  have comparable magnitudes, the fine-scale fringes modulate the large-scale oscillations up to the plateau cutoff. However, for  $\theta = \pi$ , both the cutoff positions and tunneling factors ( $\mathcal{I}_8 \approx 2\mathcal{I}_6$ ) are rather different, so that fine-scale oscillations in Fig. 2(b) are significant only for electron energies  $E \lesssim E_{\text{cut}}^{(8)}$ , where the rates  $\Gamma_6(\mathbf{p})$  and  $\Gamma_8(\mathbf{p})$  overlap. The same considerations explain also the intracycle and intercycle modulation features of the ATI spectra for He in Figs. 2(c,d).

To estimate the period  $\Delta E$  of fine-scale oscillations analytically, we consider the interference factor  $\cos \Phi_{j,j+2}(\mathbf{p})$  in Eq. (12) and approximate the difference  $\Delta \Phi(p, \theta) \equiv \Phi_{j,j+2}(p + \Delta p, \theta) - \Phi_{j,j+2}(p, \theta)$  as follows:

$$\Delta \Phi(p, \theta) \approx \frac{d\Phi_{j,j+2}}{dp} \Delta p \approx \frac{d\Phi_{j,j+2}}{dp} \frac{m\Delta E}{p}. \quad (18)$$

On the other hand, since  $\Delta \Phi(p, \theta) = 2\pi$  for two adjacent fine-scale peaks, the use of Eqs. (13) and (18) gives:

$$\begin{aligned} \Delta E &\approx 2\pi\hbar/\Delta T, \quad \Delta T = \Delta t_{\text{cl}} + \Delta t_{\text{dis}} + \Delta t_{\text{W}}, \quad (19) \\ \Delta t_{\text{cl}} &= t_r^{(j+2)} - t_r^{(j)}, \quad \Delta t_{\text{dis}} = \frac{|e|}{cp} \int_{t_r^{(j)}}^{t_r^{(j+2)}} A(t) dt, \\ \Delta t_{\text{W}} &= \frac{m\hbar}{p} \left[ \frac{d\psi(\mathbf{p} - \Delta \mathbf{p}_{j+2})}{dp} - \frac{d\psi(\mathbf{p} - \Delta \mathbf{p}_j)}{dp} \right], \end{aligned}$$

where the classical times  $\Delta t_{\text{cl}}$  and  $\Delta t_{\text{dis}}$  are the difference between two rescattering times and the laser-induced “displacement” time [3], while  $\Delta t_{\text{W}}$  has a quantum origin: it is the difference between the Wigner-like time delays [20] for the first and second rescattering events.

Our results for  $\mathcal{P}(\mathbf{p})$  are very general and applicable to any atom for which either theoretical or experimental data on the field-free DCS  $\sigma(\mathbf{p})$  and the phase  $\psi(\mathbf{p})$  of the EES amplitude are available. Since our analytic derivations were carried out in the tunneling regime, the general condition for validity of Eq. (5) for  $\mathcal{P}(\mathbf{p})$  is that the Keldysh parameters  $\tilde{\gamma}_j$  for all contributing half-cycles should be less than unity ( $0.56 \leq \tilde{\gamma}_j \leq 0.83$  in our results

for H, while  $0.67 \leq \tilde{\gamma}_j \leq 0.99$  for He). Our derivations show clearly that  $\mathcal{P}(\mathbf{p})$  cannot in general be factorized because the term  $\Delta \mathbf{p}_j = -|e|\mathbf{A}(t_r^{(j)})/c$  in Eq. (7) is sensitive to  $j$ . [Moreover, owing to the dependence of  $\mathcal{P}_{\text{int}}(\mathbf{p})$  on  $\psi(\mathbf{p} - \Delta \mathbf{p}_j)$ ,  $\mathcal{P}(\mathbf{p})$  is more sensitive to the atomic dynamics than for a monochromatic field.] Nevertheless, factorization of  $\mathcal{P}(\mathbf{p})$  can occur for a few-cycle pulse [as, e.g., in Fig. 1(b)], when only a single rate  $\Gamma_j(\mathbf{p})$  contributes predominantly to  $\mathcal{P}(\mathbf{p})$ . However, in this case, the CEP-dependent “half-cycle” EWPs  $w_j = \mathcal{I}_j \mathcal{W}_j$  are different for electrons with  $p_{\parallel} > 0$  and  $p_{\parallel} < 0$ . The factorization postulated in Ref. [11] follows from our results upon replacing  $\Delta \mathbf{p}_j$  in  $\sigma(\mathbf{p} - \Delta \mathbf{p}_j)$  in Eq. (7) and in the phase  $\psi(\mathbf{p} - \Delta \mathbf{p}_j)$  in Eq. (13) by that for the half-cycle with maximum cutoff energy  $E_{\text{cut}}^{(j)}$ , i.e., with maximum value of  $|\mathbf{A}(t_r^{(j)})|$ . [After such replacement, Eq. (5) takes a factorized form and provides an explicit expression of the EWP in this case.] However, since the DCS  $\sigma(\mathbf{p})$  usually decreases with increasing  $p$ , this approximate factorization overestimates the contribution of interfering half-cycles with smaller cutoff energies  $E_{\text{cut}}^{(j)}$ , as the upper curve in Fig. 3 shows; the lower (exact) curve agrees well with TDSE results (not shown). For  $E > 140$  eV, the exact and approximate results for  $\mathcal{P}(\mathbf{p})$  in Fig. 3 coincide since the *single* ionization amplitude,  $\mathcal{A}_{j=4}(\mathbf{p})$ , is dominant. Thus in this energy region the result (5) for  $\mathcal{P}(\mathbf{p})$  indeed reduces to a factorized form with the EWP  $w_4 = \mathcal{I}_{j=4} \mathcal{W}_{j=4}$ , while for  $E < 140$  eV the interference between amplitudes  $\mathcal{A}_{j=4}(\mathbf{p})$  and  $\mathcal{A}_{j=6}(\mathbf{p})$  becomes significant and such factorization is not possible.

To conclude, we have derived quantum-mechanically an analytic result for the ATI probability  $\mathcal{P}(\mathbf{p})$  that is valid in the high-energy part of the ATI plateau for a short laser pulse of any shape and duration. These results allow one to describe analytically the left-right asymmetry as well as the large-scale (intracycle) and fine-scale (intercycle) oscillations in ATI spectra. To use our results, only the EES amplitude  $f(\mathbf{p})$  for the target atom and the solutions  $(t_i^{(j)}, t_r^{(j)})$  of the classical equations (4) for a given short pulse are needed. Our results agree well with TDSE results and provide an efficient tool for the quantitative description of short-pulse ATI spectra.

This work was supported in part by RFBR Grant Nos. 10-02-00235 and 12-02-00064, by the Russian Federation Ministry of Education and Science, by NSF Grant No. PHY-0901673, and by NNSFC Grant Nos. 11174016, 10974007, and 11121091. Calculations at MSU were performed on the SKIF “Chebyshev” supercomputer.

\* manakov@phys.vsu.ru

† alexander.m.popov@gmail.com

‡ liangyou.peng@pku.edu.cn

§ astarace1@unl.edu

- [1] G.G. Paulus *et al.*, Phys. Rev. Lett. **91**, 253004 (2003).  
[2] F. Lindner *et al.*, Phys. Rev. Lett. **95**, 040401 (2005).

- [3] D.B. Milošević, G.G. Paulus, D. Bauer, and W. Becker, *J. Phys. B* **39**, R203 (2006).
- [4] M. Okunishi *et al.*, *Phys. Rev. Lett.* **100**, 143001 (2008); D. Ray *et al.*, *ibid.*, **100**, 143002 (2008).
- [5] T. Morishita, A.-T. Le, Z. Chen, and C.D. Lin, *Phys. Rev. Lett.* **100**, 013903 (2008).
- [6] C.D. Lin, A.-T. Le, Z. Chen, T. Morishita, and R. Lucchese, *J. Phys. B* **43**, 122001 (2010).
- [7] M.V. Frolov, N.L. Manakov, and A.F. Starace, *Phys. Rev. A* **79**, 033406 (2009).
- [8] A. Čerkić, E. Hasović, D.B. Milošević, and W. Becker, *Phys. Rev. A* **79**, 033413 (2009).
- [9] D.B. Milošević, A. Čerkić, B. Fetić, E. Hasović, and W. Becker, *Laser Phys.* **20**, 573 (2010).
- [10] O.I. Tolstikhin, T. Morishita, and S. Watanabe, *Phys. Rev. A* **81**, 033415 (2010).
- [11] S. Mischeau, Z. Chen, A.-T. Le, J. Rauschenberger, M.F. Kling, and C.D. Lin, *Phys. Rev. Lett.* **102**, 073001 (2009).
- [12] M.V. Frolov, N.L. Manakov, A.A. Silaev, N.V. Vvedenskii, and A.F. Starace, *Phys. Rev. A* **83**, 021405(R) (2011).
- [13] N.L. Manakov, V.D. Ovsiannikov, and L.P. Rapoport, *Phys. Rep.* **141**, 319 (1986).
- [14] M.V. Frolov, N.L. Manakov, E.A. Pronin, and A.F. Starace, *Phys. Rev. Lett.* **91**, 053003 (2003); M.V. Frolov, N.L. Manakov, and A.F. Starace, *Phys. Rev. A* **78**, 063418 (2008).
- [15] B.M. Smirnov and M.I. Chibisov, *Zh. Eksp. Teor. Fiz.* **49**, 841 (1965) [*Sov. Phys. JETP* **22**, 585 (1966)].
- [16] I.A. Burenkov, A.M. Popov, O.V. Tikhonova, and E.A. Volkova, *Laser Phys. Lett.* **7**, 409 (2010); A.M. Popov, O.V. Tikhonova, and E.A. Volkova, *Laser Phys.* **21**, 1593 (2011).
- [17] H.G. Muller, *Laser Phys.* **9**, 138 (1999); L.-Y. Peng and A.F. Starace, *J. Chem. Phys.* **125**, 154311 (2006).
- [18] L.-Y. Peng, E.A. Pronin, and A.F. Starace, *New. J. Phys.* **10**, 025030 (2008).
- [19] S.P. Goreslavskii and S.V. Popruzhenko, *J. Phys. B* **32**, L531 (1999).
- [20] E.P. Wigner, *Phys. Rev.* **98**, 145 (1955).